Mechanical behaviour predictions of nonlinear viscoelastic composite materials by a homogenisation of random mixtures approach

Martin Lévesque[*1], Katell Derrien[*], Leon Mishnaevski Jr.[**], Didier Baptiste[*] and Michael D. Gilchrist[***]

[*]Laboratoire LM3, ENSAM, UMR 800 CNRS 8006, 151 Boulevard de l'Hôpital, 75013 Paris, France
[**]University of Stuttgart, Materials Testing Institute, Pfaffenwaldring 32, D-70569 Stuttgart, Germany
[***]Dept. Mech. Eng., University College Dublin, Belfield, Dublin 4, Ireland

ABSTRACT

In this paper we develop a homogenisation model for nonlinear viscoelastic materials. The first step of the approach is to introduce a proper linearisation of the nonlinear phases. Secondly, the correspondence principle is used to solve the homogenisation problem. Finally, the inverse Laplace transform provides the time domain mechanical properties of the homogenised material. The predictions of this homogenised model were compared against 3D finite element simulations and good agreement was observed.

1. INTRODUCTION

The homogenisation approach allows the global mechanical behaviour of heterogeneous materials to be predicted from the knowledge of the microstructure morphology and the mechanical behaviour of each constituent phase. The approach has been widely applied to linear elastic materials with reasonable success (see [1] for a review). It has also been extended to nonlinear behaviour (plastic, elastoplastic, etc.) by linearisation of each constituent's behaviour law (see [2] for a review). Linear viscoelastic materials can also be homogenised using the correspondence principle and Laplace-Carson transforms (see [3] for a review). In both cases, the nonlinear or time dependent problem, with an appropriate treatment, is transformed into a problem that can be solved as a linear elastic one. This treatment is known as *linearisation.*

In this paper, we model the behaviour of a glass bead reinforced polypropylene. The glass is assumed to be linear elastic and isotropic while the polypropylene is nonlinear viscoelastic and also isotropic. The mechanical properties of the constituents are first presented in the next section. Then, the linearisation procedure is presented and implemented into the Mori-Tanaka scheme. The predictions of this model are compared with FE simulations of the microstructure.

2. MECHANICAL BEHAVIOUR OF THE CONSTITUENT PHASES

The polypropylene is assumed to obey the well known Schapery behaviour law, generalised in 3D according to Zhang *et al.* [4], of the form:

$$\boldsymbol{\varepsilon}^{SCHA}(t) = D_0 g_0(\sigma_e)\mathbf{S}^{\mathbf{e}} : \boldsymbol{\sigma}(t) + g_1(\sigma_e)\int_0^t \Delta D\left(\int_\tau^t \frac{d\xi}{a(\sigma_e)}\right)\mathbf{S}^{\mathbf{c}} : \frac{d}{d\tau}\left(g_2(\sigma_e)\boldsymbol{\sigma}(\tau)\right)d\tau \quad (1)$$

[1] Corresponding author. email : martin.levesque@paris.ensam.fr

where D_0 is the instantaneous compliance, g_0, g_1, g_2 and a are scalar functions of an equivalent stress σ_e, $\Delta D(t)$ is a linear viscoelastic creep compliance and the tensors $\mathbf{S}^e$ and $\mathbf{S}^c$ are fourth order tensors containing the elastic and creep Poisson's ratios. The two tensors have the form:

$$\mathbf{S}^i = \begin{bmatrix} 1 & -\upsilon_i & -\upsilon_i & 0 & 0 & 0 \\ -\upsilon_i & 1 & -\upsilon_i & 0 & 0 & 0 \\ -\upsilon_i & -\upsilon_i & 1 & 0 & 0 & 0 \\ 0 & 0 & 0 & 1+\upsilon_i & 0 & 0 \\ 0 & 0 & 0 & 0 & 1+\upsilon_i & 0 \\ 0 & 0 & 0 & 0 & 0 & 1+\upsilon_i \end{bmatrix} \quad (2)$$

In this study, it is assumed that these two Poisson's ratios are constant. The equivalent stress is given by:

$$\sigma_e = \sqrt{I_1^2 - 3I_2} \quad (3)$$

where I_1 and I_2 are the first and second stress invariants. The creep compliance is chosen to be a Prony series of the form:

$$\Delta D(t) = \sum_{i=1}^{5} J_i \left(1 - \exp\left(-\frac{t}{\varphi_i} \right) \right) \quad (4)$$

The various Schapery parameters were calculated according to [5] and the detailed results can be found in [6]. It was found that five terms in the Prony series were needed to model the polypropylene with acceptable accuracy. The numerical values for these parameters are presented in Table 1 along with the linear elastic properties of the glass bead reinforcements.

Table 1 – Mechanical properties of the constituent phases

Glass (linear elastic, isotropic)

k bulk modulus (GPa)	μ shear modulus (GPa)
57.5	26.538

Polypropylene (nonlinear viscoelastic, isotropic, Schapery)

D_0 (MPa)	ν_e	ν_c	J_1 (MPa^{-1})	φ_1 (sec)
4.95×10^{-4}	0.3	0.45	7.971×10^{-5}	3.125
J_2 (MPa^{-1})	φ_2 (sec)	J_3 (MPa^{-1})	φ_3 (sec)	J_4 (MPa^{-1})
3.678×10^{-5}	31.25	2.896×10^{-5}	100.0	7.142×10^{-5}
φ_4 (sec)	J_5 (MPa^{-1})	φ_5 (sec)	$g_0(\sigma_e)$	

312.5	3.076×10^{-5}	600.0	$1+9.19\times10^{-4}\times(\sigma_e-2.5)^2\times H(\sigma_e-2.5)$

$g_1(\sigma_e)$	$g_2(\sigma_e)$	$a(\sigma_e)$
$1 + 1.03\times10^{-3}\times(\sigma_e-15)^2\times H(\sigma_e-15)$	$1 + 7.92\times10^{-3}\times\sigma_e^2$	1

$H(\sigma_e)$ is the Heaviside step function

3. LINEARISATION AND HOMOGENISATION PROCEDURES

Before treating the case of nonlinear viscoelasticity, we discuss the linearisation procedures for nonlinear elastic materials, for illustration purposes.

The goal of linearisation is to create a fictive composite material (or comparison material) where all the constituents are linear elastic but has the same mechanical response for a given load. For example, if $\mathbf{\Sigma}'_{NL}$ is applied to the nonlinear composite and the resulting average strain $\mathbf{E}'_{NL}$ results, the objective is to find a linear composite material that, when $\mathbf{\Sigma}'_L = \mathbf{\Sigma}'_{NL}$ is applied, $\mathbf{E}'_L = \mathbf{E}'_{NL}$ is obtained. Of course, if $\mathbf{\Sigma}'' \neq \mathbf{\Sigma}'$ is applied, the linear comparison material is different. The main problem is that we do not know $\mathbf{E}'_{NL}$ and thus it is not possible in general to check if $\mathbf{E}'_L = \mathbf{E}'_{NL}$ is met. However, variational principles can be used to either bound or approximate $\mathbf{E}'_{NL}$. The results of such approaches lead to linearisation procedures around a reference loading level. We clarify these concepts below.

In this paper, we have chosen to use the affine linearisation procedure suggested by Masson *et al.* [7]. The comparison material is composed of linear elastic materials with tangent properties where stress free deformation or strain free stresses are added. An example of stress free deformation is a strain due to temperature variation. Therefore, the comparison material can be related to a thermo elastic material. For example if the stresses are applied, the tangent compliance of the affine formulation is defined by:

$$\mathbf{M}_r^{tgt} = \frac{\partial^2 v}{\partial\boldsymbol{\sigma}\partial\boldsymbol{\sigma}}(\overline{\boldsymbol{\sigma}}_r) \quad (5)$$

where $\mathbf{M}_r^{tgt}$ is the tangent compliance of a given phase (matrix or reinforcements), v is a potential from which the strains are derived and $\overline{\boldsymbol{\sigma}}_r$ is the *average* stress in a given phase. The stress free deformation $\boldsymbol{\varepsilon}_r^0$ is then calculated so that:

$$\frac{\partial v}{\partial\boldsymbol{\sigma}}(\overline{\boldsymbol{\sigma}}_r) = \mathbf{M}_r^{tgt} : \overline{\boldsymbol{\sigma}}_r + \boldsymbol{\varepsilon}_r^0 \quad (6)$$

This latter condition can be graphically represented in figure 1. In this particular case, the linearisation procedure is defined by equations (5,6) and the reference level is the mean stress in a given phase.

These results which are valid for nonlinear elasticity must now be extended to account for nonlinear viscoelasticity. Instead of linearising around the mean stress, the linearisation has to be done around the mean stress *history*. A tangent linear viscoelastic material is sought so that:

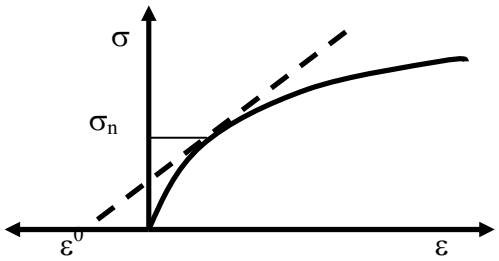

Figure 1 – Linearisation example. Solid line: real material; dotted line: linearised material

$$\boldsymbol{\varepsilon}^{SCHA}(t) = \boldsymbol{\varepsilon}^{LIN}(t) = \int_0^t \mathbf{M}(t-\boldsymbol{\tau}, t_n) : \frac{d\boldsymbol{\sigma}(\boldsymbol{\tau})}{d\boldsymbol{\tau}} d\boldsymbol{\tau} + \boldsymbol{\varepsilon}^{\mathbf{0}}(t) \qquad t \le t_n \quad (7)$$

where $\mathbf{M}(t,t_n)$ is a linear viscoelastic creep compliance, $\boldsymbol{\varepsilon}^{\mathbf{0}}$ a stress free deformation history, t_n is the time at which the solution is sought, $\boldsymbol{\varepsilon}^{SCHA}$ is the strain of the Schapery material and $\boldsymbol{\varepsilon}^{LIN}$ is the strain of the linearised material.

The definition of a tangent linear viscoelastic compliance is not as straightforward as in the case of materials described by a potential. It involves some development of the functional theory and a simple way of calculating it is not possible. We have chosen to use the approximate tangent linear viscoelastic compliance suggested by Pouya and Zaoui [8] which defines $\mathbf{M}_r^{tgt}$ so that:

$$\dot{\boldsymbol{\varepsilon}}^{SCHA}(t_n) = \dot{\boldsymbol{\varepsilon}}^{LIN}(t_n) \quad (8)$$

In this study, we have chosen to use a Maxwell solid to linearise the Schapery material. The behaviour law of such a solid is given by:

$$\boldsymbol{\varepsilon}_{SPH}^{MAX}(t) = \frac{1}{3}\int_0^t k^{-1}(t-\tau)\frac{d}{d\tau} sph\left(\boldsymbol{\sigma}(\tau)\right) d\tau \quad (9)$$

$$\boldsymbol{\varepsilon}_{DEV}^{MAX}(t) = \frac{1}{2}\int_0^t \mu^{-1}(t-\tau)\frac{d}{d\tau} dev\left(\boldsymbol{\sigma}(\tau)\right) d\tau \quad (10)$$

$$k^{-1}(t) = \alpha + \beta t \quad (11)$$

$$\mu^{-1}(t) = \gamma + \varphi t \quad (12)$$

where the *SPH* and *DEV* subscripts refer to the spherical and deviatoric parts of a tensor, the *sph(.)* and *dev(.)* operators extract the spherical and deviatoric parts of a tensor, k^{-1} and μ^{-1} are the bulk and shear compliances and α, β, γ and φ are material constants. The system of equations introduced by the combination of equations (9 - 12) leads to 2 independent equations for 4 unknowns. To close the system, an additional constraint must be added. In our case, we have chosen one of the following constraints:

$$\boldsymbol{\varepsilon}^{SCHA}(t_n) = \boldsymbol{\varepsilon}^{MAX}(t_n) \text{ (13a) or } \beta, \varphi \geq 0 \text{ (13b)}$$

Constraint (13b) comes from the condition of thermodynamic stability. It should be noted here that condition (8) can lead to an anisotropic material. In order to obtain analytical solutions of the homogenisation problem, $\mathbf{M}_r^{tgt}$ is approximated by $\mathbf{M}_r^{ISO}$ which is isotropic. $\mathbf{M}_r^{ISO}$ is calculated so that condition (8) is met for at least one component of the strain tensor.

So, for our particular case, the linear viscoelastic material is calculated by the system of equations formed by conditions (8) and (13a). If the solution leads to constants that satisfy condition (13b), the constants are kept. If condition (13b) is not met, the linearisation is done by imposing conditions (8) and (13b). Once $\mathbf{M}^{\mathbf{ISO}}$ has been identified, $\boldsymbol{\varepsilon}^{\mathbf{0}}$ is calculated according to (7).

3.1 Homogenisation

With the linearisation described in the previous section, the homogenisation problem becomes a linear viscoelastic problem where the various phases of the material are subjected to a stress free deformation history. Thanks to the Laplace-Carson transforms, this problem can be treated as a linear elastic problem with a stress free deformation. Since the simulated material is a dominant phase (i.e., matrix) in which randomly distributed spherical reinforcements are embedded, the Mori-Tanaka scheme [9,10] has been chosen for the homogenisation. This type of microstructure leads to a globally isotropic material, allowing treatment of the deviatoric and spherical parts separately. For this microstructure, the homogenised bulk and shear compliances are [11]:

$$\widetilde{\mathbf{S}} = \left\{\widetilde{k}^{-1}, \widetilde{\mu}^{-1}\right\} = \left\{\frac{(1-c_1)(k_0 + \varpi_0(k_1 - k_0)) + c_1 k_0}{k_0\left[(1-c_1)(k_0 + \varpi_0(k_1 - k_0)) + c_1 k_1\right]}, \frac{(1-c_1)(\mu_0 + \zeta_0(\mu_1 - \mu_0)) + c_1 \mu_0}{\mu_0\left[(1-c_1)(\mu_0 + \zeta_0(\mu_1 - \mu_0)) + c_1 \mu_1\right]}\right\}$$

$$\varpi_0 = \frac{3k_0}{3k_0 + 4\mu_0} \qquad \zeta_0 = \frac{6(k_0 + 2\mu_0)}{5(3k_0 + 4\mu_0)} \quad (14)$$

where $\widetilde{k}^{-1}$ and $\widetilde{\mu}^{-1}$ are the homogenised bulk and shear compliances, the subscripts 0 and 1 refer to the matrix and the reinforcement respectively and c is a volume fraction. When the various phases are subjected to a stress free deformation, the resulting macroscopic strain is given by:

$$\mathbf{E}^0 = \left\langle \mathbf{B}_i^T : \boldsymbol{\varepsilon}_i^0 \right\rangle \quad (15)$$

where the $\langle . \rangle$ operator calculates the spatial average of its argument, $\mathbf{B}$ is the so-called stress concentration tensor and subscripts i refers to each phase. In this specific situation, the stress free deformation in the reinforcement is zero (since no linearisation of the reinforcement is necessary), (15) becomes:

$$\mathbf{E}^0 = c_0 \mathbf{B}_0^T : \boldsymbol{\varepsilon}_0^0 \quad (16)$$

$$\mathbf{B}_0 = \left\{B^{SPH}, B^{DEV}\right\} = \left\{ \frac{k_0 + \varpi_0(k_1 - k_0)}{(1-c_1)(k_0 + \varpi_0(k_1 - k_0)) + c_1 k_1}, \frac{\mu_0 + \zeta_0(\mu_1 - \mu_0)}{(1-c_1)(\mu_0 + \zeta_0(\mu_1 - \mu_0)) + c_1 \mu_1} \right\} \quad (17)$$

where $\mathbf{B}_0$ is given in short hand Hill's notation (i.e. decomposed into spherical and deviatoric parts). The introduction of stress free deformations in the matrix induces stresses in the reinforcement and in the matrix. This induced stress is given by:

$$\boldsymbol{\sigma}_0^0 = -\mathbf{R}_0 : \boldsymbol{\varepsilon}_0^0 \quad (18)$$

$$\mathbf{R}_0 = \left\{R^{SPH}, R^{DEV}\right\} = \left\{ \frac{3c_1 k_1 k_0 (1-\varpi_0)}{(1-c_1)(k_0 + \varpi_0(k_1 - k_0)) + c_1 k_1}, \frac{2c_1 \mu_1 \mu_0 (1-\zeta_0)}{(1-c_1)(\mu_0 + \zeta_0(\mu_1 - \mu_0)) + c_1 \mu_1} \right\} \quad (19)$$

For the complete solution of all quantities involved in this homogenisation problem, refer to [11]. By the superposition principle, the stress in the matrix is the sum of the stress induced by the free stress deformation and the stress due to the mechanical loading. The stress concentration tensor allows the microscopic stress to be related to the macroscopic stress so that:

$$\boldsymbol{\sigma}_0 = \mathbf{B}_0 : \boldsymbol{\Sigma} + \boldsymbol{\sigma}_0^0 = \mathbf{B}_0 : \boldsymbol{\Sigma} - \mathbf{R}_0 : \boldsymbol{\varepsilon}_0^0 \quad (20)$$

This linear viscoelastic homogenisation problem, with a history of stress free deformation is solved as follows. Suppose that the stress history in the matrix is known over $[0, t_{n-1}]$ and the solution is sought at t_n. The first step is to assume a stress tensor at t_n and perform the linearisation. The Laplace-Carson transforms are applied to the matrix and reinforcement behaviour laws. The symbolic moduli are introduced in the homogenisation equations and the symbolic homogenisation tensors are obtained. The inverse Laplace-Carson transform is applied to these tensors in order to obtain their time-domain expressions. The stress at time t_n is calculated in the matrix. If this calculated stress is equal to the assumed stress, the solution has converged. If not, further iterations are conducted. At the end, the global response of the composite is given by these convolution integrals:

$$\mathbf{E}(t) = \int_0^t \widetilde{\mathbf{S}}(t-\tau) : \frac{d}{d\tau}\left(\boldsymbol{\Sigma}(\tau)\right) d\tau + \mathbf{E}^0(t) \quad (21)$$

$$\mathbf{E}^0(t) = c_0 \int_0^t \mathbf{B}_0^T(t-\tau) : \frac{d}{d\tau}\left(\boldsymbol{\varepsilon}_0^0(\tau)\right) d\tau \quad (22)$$

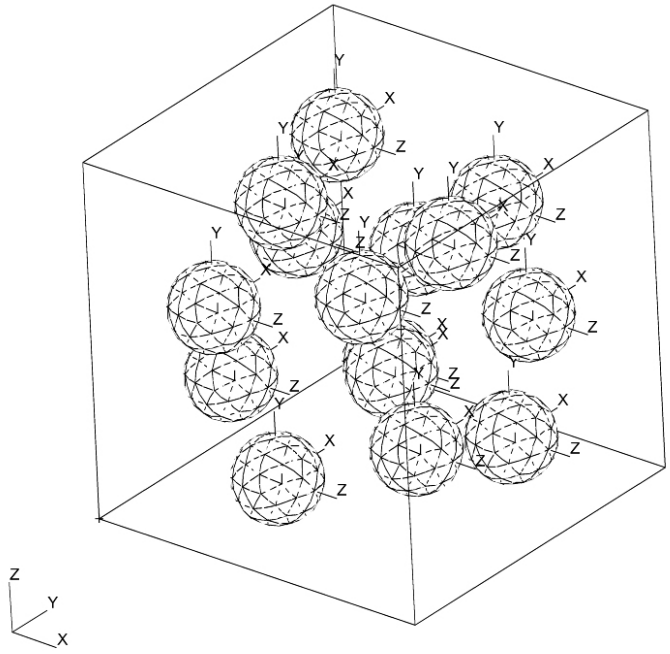

Figure 2 – 3D FE mesh of 15 glass beads randomly distributed into the matrix (not shown on the picture)

4. FINITE ELEMENT MODEL

In order to verify the theoretical model presented above, 3D numerical finite element simulations of the deformation of polymer composites with random arrangement of inclusions were carried out. The generated microstructures were placed in a box 10 x 10 x 10 mm, which was then subject to a uniaxial loading. In order to generate a microstructure with random arrangement of spherical particles, the coordinates of each particle were calculated using the uniform random number generator. Each coordinate was produced independently, with another random number seed. After the coordinates of a first particle were defined, the coordinates of each new particle were determined both by using the random number generator, and from the condition that the distance between the new particle and all adjacent particles is no less than 0.2 of the given particle radius. If the condition is not met, the seed of the random number generator is changed, and the coordinates of the new particle are recalculated. In order to avoid the boundary effects, the distance between a particle and borders of the box is required to be no less than 0.1 particle radius. See figure 2.

The maximum number of particles that was possible to account for was 15 (restriction imposed by the required memory to perform the calculations). A UMAT

subroutine has been written for the Schapery material and the properties used for the glass can be found in table 1.

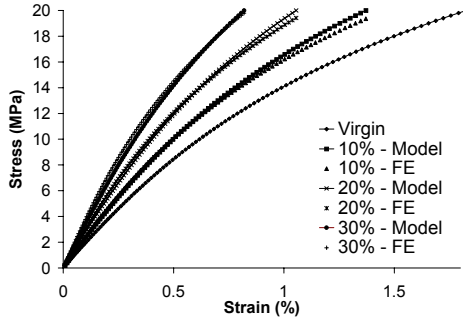

Figure 3 – Model and FE simulations of a tensile loading of 1 MPa / s for various volume fractions of glass bead reinforcement

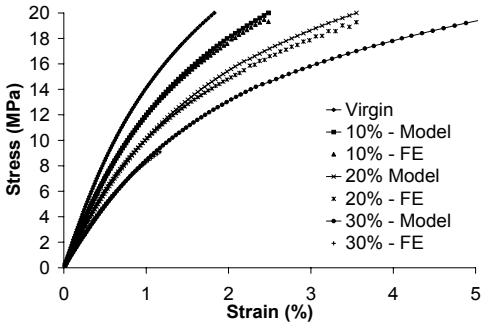

Figure 4 – Model and FE simulations of a tensile loading of 1 MPa / s for various volume fractions voids

5. MODEL / FINITE ELEMENT COMPARISONS

In order to assess the validity of the model, the following aspects were studied: 1) Effect of reinforcement volume fraction and contrast and 2) Sensitivity to the loading rate. For each aspect, the predictions from the model and from the FE simulations were compared for uniaxial loading. For each simulation, the stress history was a constant loading rate from 0 to 20 MPa.

Effect of volume fraction and contrast

Figure 3 shows the comparison between the FE results and the model developed in this paper. For all the volume fractions of reinforcements, the agreement is quite good.

The sensitivity of the model to the mechanical properties contrast is studied by simulating a porous material of the same volume fractions as the reinforced one. Figure 4 shows the stress – strain curves for various volume fractions of pores. It should be noted that convergence problems were encountered with the FE simulations for the 30 % void content and therefore the results are not presented for the whole stress-strain curve. These numerical difficulties are still under investigation. For the simulated cases, the agreement is good.

Effect of the loading rate

Figure 5 shows the stress – strain curves obtained for a 20% glass beads reinforced polypropylene loaded at different stress rates. The load histories were a constant stress rate from 0 to 20 MPa. The figure shows that the model takes into account the material sensitivity to the load rate since a faster load rate leads to a stiffer material. Here again the predictions given by the model agree well with the finite element simulations.

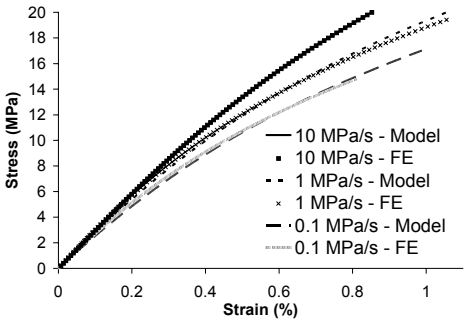

Figure 5 – Effect of the loading rate on the mechanical response of a 20 % glass bead reinforced polypropylene submitted to a constant stress rate tensile loading, for various stress rates

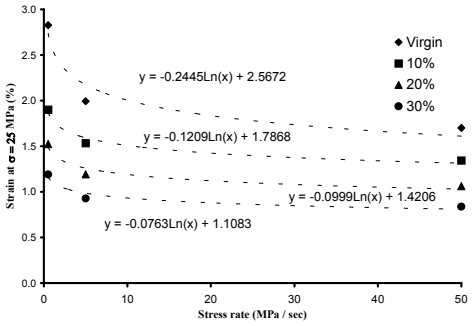

Figure 6 – Strain at $\sigma = 25$ MPa tensile loading at a constant stress rate, for various stress rates and reinforcement volume fractions

Figure 6 shows the strain predicted by the model for a stress of 25 MPa for various stress rates and volume fractions of reinforcement. A logarithmic curve fit of the simulated data has been done for every volume fraction of reinforcement. It can be observed that a stress rate variation has a greater effect on the strain at 25 MPa as the volume fraction of reinforcement decreases. These tendencies are expected in a real material since as the volume fraction of linear elastic particles increases, the global behaviour of the composite tends towards the behaviour of an elastic material.

6. CONCLUSION

A homogenisation model for simulating the mechanical behaviour of a nonlinear viscoelastic material has been developed. For the volume fractions and the loading simulated, this model provides acceptable results when compared with finite element simulations. It has also been shown that the approximation $\mathbf{M} \approx \mathbf{M}^{\mathbf{ISO}}$ is reasonable. However it is expected that the discrepancy in the results obtained with $\mathbf{M}$ and $\mathbf{M}^{\mathbf{ISO}}$ will increase as the degree of nonlinearity increases. The limitations of such simplification must be studied. In addition, a more refined calculation of $\mathbf{M}^{\mathbf{ISO}}$ could be developed.

The model takes into account the viscoelastic characteristics of the homogenised composite material. It has been shown, for example, that the homogenised material is sensitive to the loading rate.

Comparison of the model predictions vs FE simulations shows good agreement. This finding will be useful when experimental validation of the model will be conducted on real materials. This observation decreases the number of factors that would cause any discrepancy between the model and the experiments.

REFERENCES

[1] **Tucker, C.L., Liang, E**., "Stiffness predictions for unidirectional short-fiber composites: Review and evaluation", *Composites Science and Technology,* **59** (1999), 655 - 671.

[2] **Masson, R., Zaoui, A.**, "Self-consistent estimates for rate-dependant elastoplastic behaviour of polycrystalline materials", *J. Mech. Phys. Solids*, **47 (**1999), 1543 – 1568.

[3] **Brinson, L.C., Lin, W.S.**, "Comparison of micromechanics methods for effective properties of multiphase viscoelastic composites", *Composites Structures*, **41** (1998), 353 – 367.

[4] **Zhang, L., Ernst, L.J., Brouwer, H.R.**, "A study of nonlinear viscoelasticity of an unsaturated polyester resin. Part 2. 3D model", *Mechanics of materials*, **26** (1997), 167 – 195.

[5] **Papanicolaou, G.C., Zaoutsos, S.P. and Cardon,A.H.**, "Further development of a data reduction method for the nonlinear viscoelastic characterization of FRPs", *Composites part A*, **30** (1999), 839 – 848.

[6] **Marques, G.**, "Prédiction du comportement mécanique d'un polymère", Final year project internal report (French), Ecole Nationale Supérieure d'Arts et Métiers, Paris, France, 2003.

[7] **Masson, R., Bornert, M., Suquet, P., Zaoui, A.**, "An affine formulation for the prediction of the effective properties of nonlinear composites and polycrystals", *J. Mech. Phys. Solids,* **48 (**2000), 1203 – 1227.

[8] **Pouya, A., Zaoui, A.,** "Linéarisation et homogénéisation en viscoélasticité", *C.R. Acad. Sci. Paris, t. 327 Série II b* (1999), 365 – 370.

[9] **Mori, T., Tanaka, K.**, "Average stress in matrix and average elastic energy of materials with misfitting inclusions", *Acta metallurgica*, **21** (1973), 571 – 574.

[10] **Benveniste, Y.**, "A new approach to the application of Mori-Tanaka's theory in composite materials. Mechanics of materials", **6 (**1987), 147 – 157.

[11] **Bourgeois, N.**, "Caractérisation et modélisation micromécanique du comportement et de l'endommagement d'un composite à matrice métallique : Al/SiCp". Ph.D. Thesis (French) Ecole Centrale Paris, Paris, France, 1994.